

Dissipation control based on differences between
numerical and physical fluxes
ADIGMA deliverable 3.3.6
Version 1.0



September 30, 2009

Contents

1	UNBG Results	3
1.1	UNBG Strategy	3
1.1.1	UNBG Shock Capturing Approach	3
1.1.2	Troubled Cell Indicators	6
1.2	Numerical results	6
1.2.1	General Settings	6
1.2.2	1D Test Cases	6
1.2.3	2D Test Cases	7
1.3	Summary	10

1

UNBG Results

Francesco Bassi, Alessandro Colombo, Nicoletta Franchina, Stefano Rebay, UNBG

1.1 UNBG Strategy

The UNBG strategy for the control of oscillations of DG methods is similar in the spirit to the SUPG shock-capturing technique analyzed in [5]. As such, the method explicitly adds an artificial viscosity term to the governing equations and controls the amount of added viscosity by means of a residual-based viscosity coefficient. First forms of this approach were presented already in [1, 2] and a similar technique, with a different choice for the residual-based viscosity coefficient, was also used by Hartmann and Houston in [4] and presented in much greater detail by Hartmann in [3].

1.1.1 UNBG Shock Capturing Approach

The shock-capturing approach developed by UNBG aims at controlling the oscillations of high order approximations of discontinuous solutions while preserving as much as possible the spatial resolution of discontinuities, i.e., it aims at achieving sub-cell resolution of discontinuities. The form of the shock-capturing term employed by UNBG has developed over the years, mainly on the basis of physical arguments and numerical experiments, trying to balance several conflicting requirements, such as accuracy, robustness and no need of case-specific fine tuning of parameters. Unlike other shock-capturing approaches employed in DG methods, the UNBG approach does not use a troubled cell indicator to detect elements where artificial viscosity is needed. The shock-capturing term is active in every element, but the amount of artificial viscosity is proportional to the residual of the DG space discretization and thus it is everywhere negligible except than in elements containing shocks. Former versions of the shock-capturing term set the amount of artificial diffusion proportional to the value of an element-wise function s , which is actually the lifting of the jumps between the inviscid numerical flux and the normal component of the

internal one. The DG discretization is thus modified by introducing the following term:

$$\sum_K \alpha \int_K \epsilon_k(\mathbf{u}_h^\pm) \partial_{xi} u_h^k \partial_{xi} v_h^k \, d\mathbf{x} \quad (1.1)$$

with the shock sensor defined as follows

$$\epsilon_k(\mathbf{u}_h^\pm) = \frac{Ch_K^2 |s_k(\mathbf{u}_h^\pm)|}{u_s^k(\mathbf{u}_h)}, \quad (1.2)$$

and

$$\int_K v_h^k s_k(\mathbf{u}_h^\pm) \, d\mathbf{x} = \int_{\partial K} v_h^k \left(\widehat{\mathbf{f}}_c(\mathbf{u}_h^-, \mathbf{u}_h^+, \mathbf{n}^-) - \mathcal{F}_c(\mathbf{u}_h) \cdot \mathbf{n}^- \right)_k \, d\sigma, \quad (1.3)$$

where $\widehat{\mathbf{f}}_c(\mathbf{u}_h^-, \mathbf{u}_h^+, \mathbf{n}^-)$ is the numerical flux function and $\mathcal{F}_c(\mathbf{u}) \cdot \mathbf{n}$ the internal one. The index k in the above equations is introduced to denote the k -th component of the unknown solution vector \mathbf{u}_h . The viscosity coefficients defined in eq. (1.5) can be regarded as a diagonal viscosity matrix and as such they do not provide any coupling of the artificial viscosity terms in the different equations. The vector \mathbf{u}_s has been introduced both for dimensional reasons and in order to provide a proper scaling of the viscosity coefficients in the different equations. In former 2D computations \mathbf{u}_s was chosen as:

$$\mathbf{u}_s = \begin{bmatrix} \rho \\ \rho e_0 \\ \rho \sqrt{2e_0} \\ \rho \sqrt{2e_0} \end{bmatrix}. \quad (1.4)$$

The shock capturing coefficient described above has shown some weaknesses. First the laplacian nature of the artificial viscous term introduced an isotropic diffusivity. Furthermore the method was not robust enough due to the difficulty of achieving a well balanced magnitude of the viscosity coefficient ϵ_k . Finally, for very high order (higher than 2^{nd} or 3^{rd} order) approximation of shocks lying within elements, oscillations control based only on the function s turned out to be too weak. These shortcomings have been addressed within the ADIGMA project and led us to introduce the following modifications. The viscous like term has been made directional by applying the diffusion in the direction of the pressure gradient (locally within elements). This preserves the resolution of contact discontinuities, is physically consistent for shock waves even in 2D or 3D and does not spoil the near-wall behavior of high order solution of viscous and turbulent flows. Moreover, for very high order approximations the function s_k has been augmented with the contribution of the divergence of the inviscid flux inside elements. Considering the Euler equations, the DG discretization is therefore modified by the introduction of the following term:

$$\sum_K \alpha \int_K \epsilon_k(\mathbf{u}_h^\pm) (b_i(\mathbf{u}_h) \partial_{xi} u_h^k) (b_i(\mathbf{u}_h) \partial_{xi} v_h^k) \, d\mathbf{x} \quad (1.5)$$

$\frac{\partial \hat{p}}{\partial \epsilon} + 7. (p55)$

Residual strong form

with the shock sensor and the pressure based unit vector defined as follows

$$\epsilon_k(\mathbf{u}_h^\pm) = \frac{Ch_K^2 (|s_k(\mathbf{u}_h^\pm)| + |\text{div}(\mathcal{F}_c(\mathbf{u}_h))_k|)}{u_s^k(\mathbf{u}_h)} \quad \mathbf{b}(\mathbf{u}_h) = \frac{\nabla p(\mathbf{u}_h)}{|\nabla p(\mathbf{u}_h)| + \varepsilon}. \quad (1.6)$$

A matrix form of the viscosity coefficients for the shock-capturing term of a DG method was already proposed in [5], while the form employed by [6] in an explicit SD method was simply diagonal. After a few numerical experiments with matrix forms of viscosity coefficients, we found that the shock-capturing scheme displayed a more robust and accurate behavior using the same scalar ϵ_q for each component of \mathbf{u}_h . A simple and effective way to combine the components of \mathbf{s} into the single function s_q for a generic quantity q (this could be any desired quantity derived from \mathbf{u}_h) is the following:

$$s_q(\mathbf{u}_h^\pm) = \sum_k \frac{\partial q(\mathbf{u}_h)}{\partial u_h^k} s_k(\mathbf{u}_h^\pm). \quad (1.7)$$

Accordingly, combining also the divergence of the inviscid flux

$$d_q(\mathbf{u}_h) = \sum_k \frac{\partial q(\mathbf{u}_h)}{\partial u_h^k} \text{div}(\mathcal{F}_c(\mathbf{u}_h))_k, \quad (1.8)$$

the resulting viscosity coefficient ϵ_q reads:

$$\epsilon_q(\mathbf{u}_h^\pm) = \frac{Ch_K^2 (|s_q(\mathbf{u}_h^\pm)| + |d_q(\mathbf{u}_h)|)}{|q(\mathbf{u}_h)|}. \quad (1.9)$$

For aerodynamic flows the pressure p can be considered a quite natural choice for q . The shock-capturing term of eq. (1.5), with each ϵ_k replaced by the ϵ_q of eq. (1.9), allows a satisfactory control of oscillations, but it also slightly affects the accuracy of solutions in regions with high but otherwise smooth gradients. A further improvement in this respect has been achieved by making ϵ_q more selective by means of the factor f_p defined by:

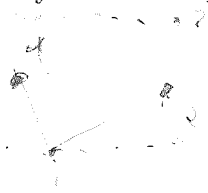
$$f_p = \frac{|\nabla p|}{p} \left(\frac{h_K}{P+1} \right), \quad (1.10)$$

where P defines the degree of the polynomial approximation. With this final modification the shock-capturing term introduces an amount of artificial viscosity that both preserves the accuracy within smooth flow regions and allows crisp representation of shock profiles. Moreover, the numerical evidence indicates that the user-defined coefficient α can take almost the same value when using different degrees of polynomial approximation. As a matter of fact, we have used $\alpha = 0.2$ in all of the following computations.

Finally, the element dimension h_K is defined as

$$h_K = \frac{1}{\sqrt{\frac{1}{(\Delta x)^2} + \frac{1}{(\Delta y)^2} + \frac{1}{(\Delta z)^2}}}, \quad (1.11)$$

where $\Delta x, \Delta y$ and Δz are the dimensions of the hexahedral enclosing K , scaled in such a way that their product matches the volume of K .



5



Tri: $\mathcal{B}_2(N_2 - N_1)$
Quad: $\mathcal{B}_2(N_2 - N_1, N_3 - N_1)$

Hex: $\mathcal{B}_2(N_2 - N_1, N_3 - N_1, N_4 - N_1)$

1.1.2 Troubled Cell Indicators

As already mentioned in Sec. 1.1.1 the UNBG approach does not implement a strategy to mark the elements where the artificial viscosity will be switched on or off. Instead, UNBG effort focused on the construction of a shock-capturing term capable of accurately balancing the amount of artificial viscosity so as to control oscillations around shocks without affecting the accuracy in smooth, high-gradient, flow regions.

1.2 Numerical results

1.2.1 General Settings

The results of the Burgers equation presented in the following have been obtained using ∇u in place of ∇p and $p = 1$ in eq. 1.10. The 1D Euler solutions have been computed using $q = p$. The shock-capturing term outlined above will be used to stabilize high order DG solutions containing discontinuities in inviscid, viscous and turbulent multidimensional flows. We remark that for turbulent computations the shock-capturing term is used only in the mean flow equations. Finally we note that the shock-capturing term must be treated implicitly (at least for the part of $\partial_{xi} u_h^k$) also in explicit computations. Moreover, in our experience the highly non-linear character of the shock-capturing term requires a fully linearized implicit treatment for the convergence of residuals in steady state computations.

1.2.2 1D Test Cases

The 1D results presented in this section highlight the role of the functions s_q and d_q in controlling the shock resolution and the damping of oscillations around discontinuities. For this purpose we have solved the 1D inviscid Burgers equation with two different sets of initial conditions. In the first case, starting from an initial sinusoidal wave $f = \sin(2\pi x)$ centered within the domain $[0, 1]$, the solution develops a discontinuity, that, using an odd number of grid elements, lies within the central element. In order to highlight the shock resolution of the scheme the solutions of the following figures have been represented using $P + 1$ nodes within each element.

The Figures 1.1–1.3 display the \mathbb{P}_5 and \mathbb{P}_{19} solutions at $t = 0.6$, computed using an explicit TVD Runge-Kutta scheme. The solutions reported in the Figures 1.1(a) and 1.1(c) have been computed switching off the s_q and d_q contributions, respectively. The comparison clearly shows that for the higher-order accurate approximations a shock-capturing approach exclusively based upon the “lifting” function of interface flux jumps is not completely satisfactory. Even increasing two or three times the amount of artificial viscosity by means of the user-defined coefficient α does not help in reducing the oscillations, as shown in Figure 1.1(b). Instead, for very high order approximations and for discontinuities lying within elements, it has been found that the inviscid flux divergence internal to the elements can be more effective to control the oscillations. In fact, for the higher order approximations

the d_q term was found to give the major contribution in defining sharp shock profiles free of oscillations, as the comparison between Figure 1.1(c) and 1.1(d) shows.

Numerical investigations have also shown that the factor f_p defined by eq. (1.10) significantly improves the sub-cell resolution of shocks within elements without affecting the accuracy in regions of smooth flow. This scaling factor effectively discriminates high but otherwise continuous (pressure) gradients from the high gradients associated with discontinuities. In this way it also contributes in reducing the well known spurious entropy productions that usually take place around the leading edge of airfoils. Finally, scaling the factor f_p with the polynomial degree ensures a resolution of discontinuities over the same number of plotting points (as defined above), i.e., an increasingly higher space resolution. This result has been achieved without any fine tuning of the parameter α that has been kept constant for all the flow solutions. The effect of the increased space resolution of discontinuities rising the polynomial approximation can be appreciated from Figure 1.3. From our numerical experience all the remarks mentioned above apply to polynomial approximations ranging from 5-6 up to 19, see the Figure 1.2 displaying the results on the same tests using \mathbb{P}_5 elements.

The Figure 1.4 shows the unsteady \mathbb{P}_5 and \mathbb{P}_{19} solutions of the Burgers equation computed at $t = 0.6$ using an explicit TVD Runge-Kutta scheme, starting from an initial sinusoidal wave $f = \sin(\pi x)/2 + \sin(2\pi x)$. Similarly to what happens in the steady case, also these solutions highlight that the inviscid flux divergence internal to the elements allows a better control of oscillations.

Finally the Figures 1.5, 1.6 and 1.7 show some higher-order results for a set of benchmark 1D unsteady problems. For these problems the method provides very sharp resolution of both shocks and contact discontinuities.

1.2.3 2D Test Cases

The numerical 2D computations of the DMR and MTC2 problem exploited for the assessment of the shock-capturing methodologies are reported within D3.3.14. All the computations have been performed using the same user-defined coefficient $\alpha = 0.2$. This value ensured stable solutions and crisp representation of discontinuities, but somewhat higher values would probably provide less wiggly solutions. We also remark that values around 0.2 have been used in many other computations on different test cases and different grid sizes without any stability problem. See D3.3.14.

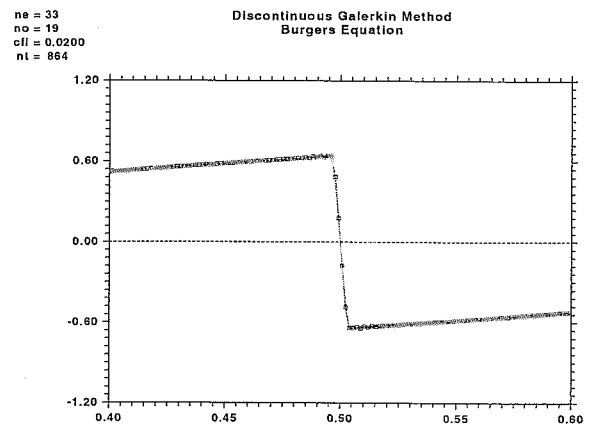
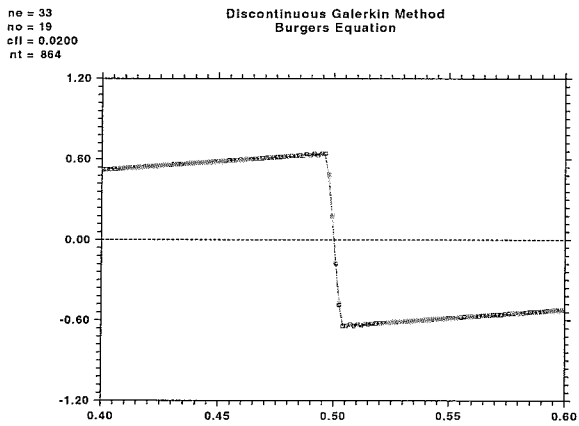
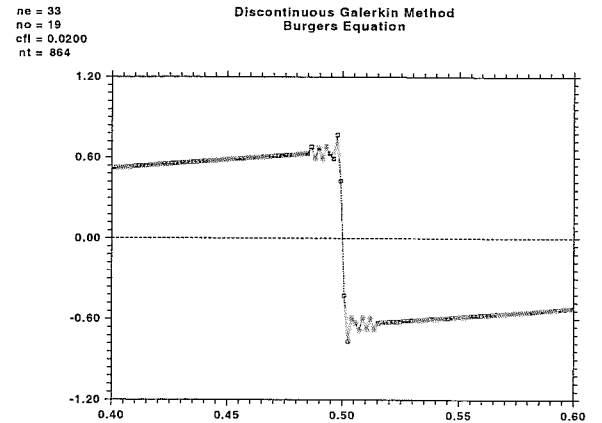
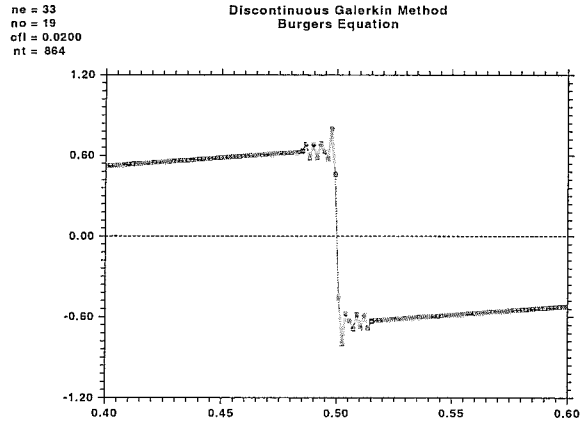


Figure 1.1: Burgers equation: \mathbb{P}_{19} solutions, zoom on the discontinuity of the 1D-domain $x = [0, 1]$ subdivided into 33 elements.

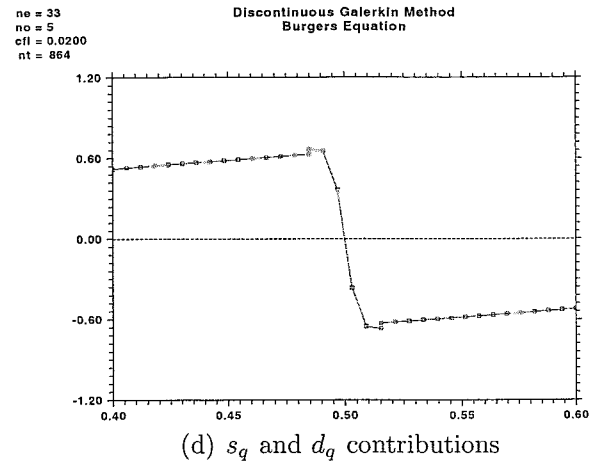
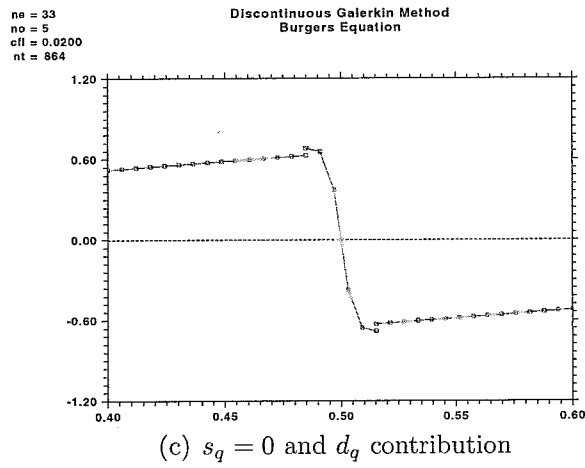
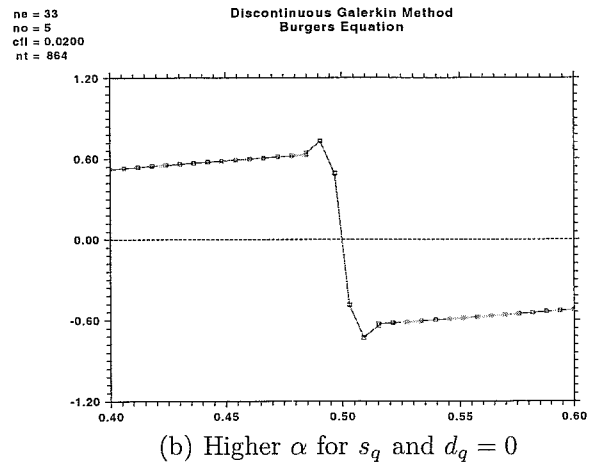
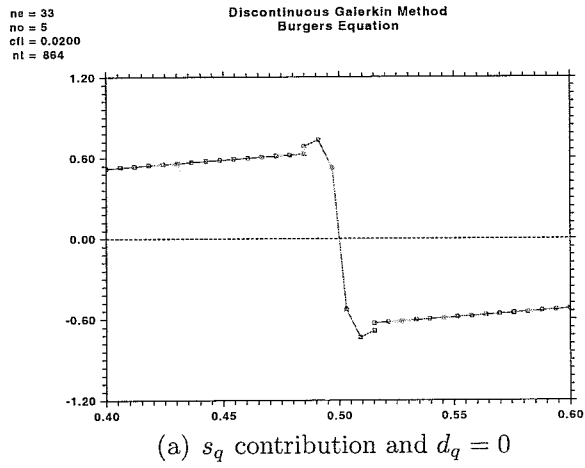


Figure 1.2: Burgers equation: \mathbb{P}_5 solutions, zoom on the 1D-domain $x = [0, 1]$ subdivided into 33 elements.

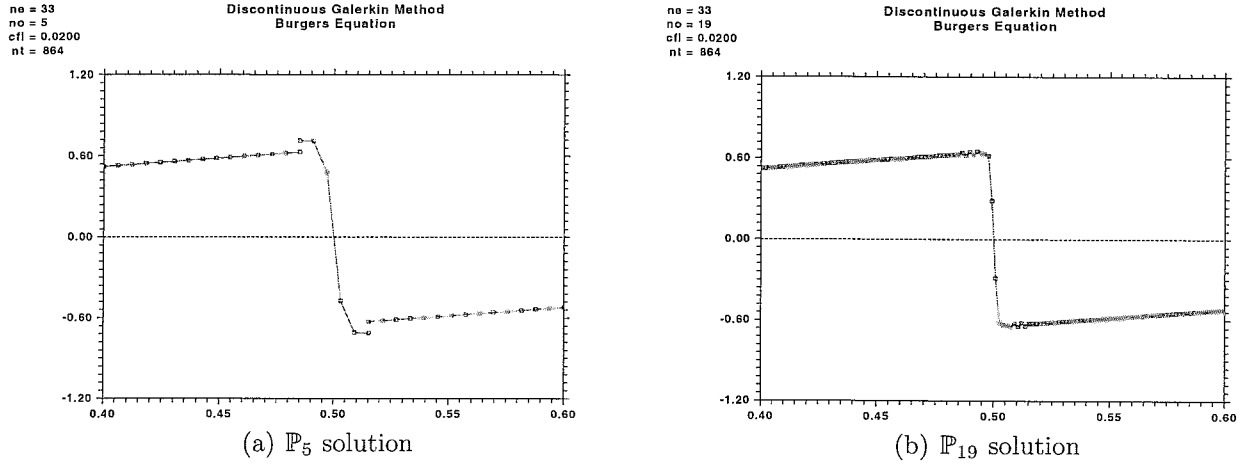


Figure 1.3: Burgers equation: zoom on the 1D-domain $x = [0, 1]$ subdivided into 33 elements when using fine tuning of the shock-capturing term (both s_q and d_q have been employed).

1.3 Summary

The shock-capturing approach for DG methods developed by UNBG aims at achieving an optimal balance among several contrasting objectives, such as accuracy, robustness and no need of case-specific fine tuning of parameters. Moreover, its applicability to steady and unsteady flows has always been considered highly desirable. Numerical investigations have shown that for high order approximations a shock capturing approach exclusively based upon the differences between the numerical and physical fluxes can not be satisfactory and requires thus the use of an additional control mechanism. For this purpose the divergence of the inviscid flux inside elements has been found suited to ensure a better control of the oscillations within the elements.

The results presented in the previous sections and in D3.3.14 show that the UNBG approach is capable of resolving with excellent accuracy both shocks and contact discontinuities. The shock-capturing approach developed by UNBG has been implemented in the framework of both explicit and implicit integration methods for the solution of the DG space discretized Euler, Navier-Stokes and RANS+ $k-\omega$ equations.

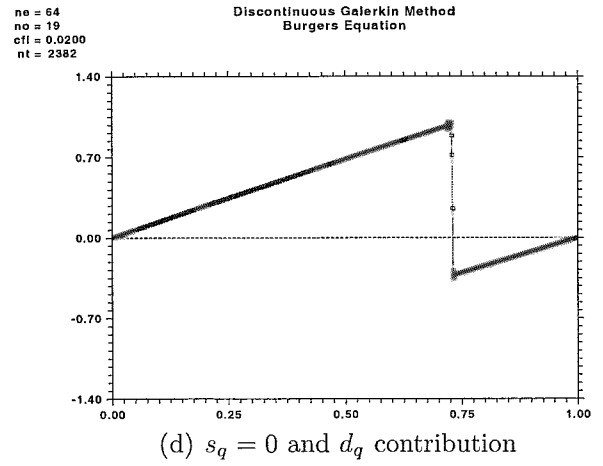
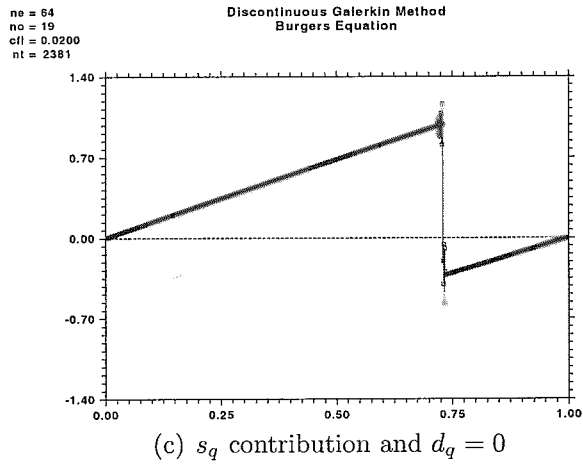
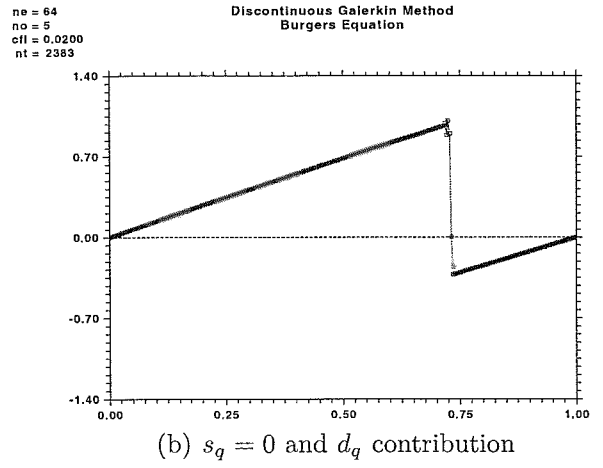
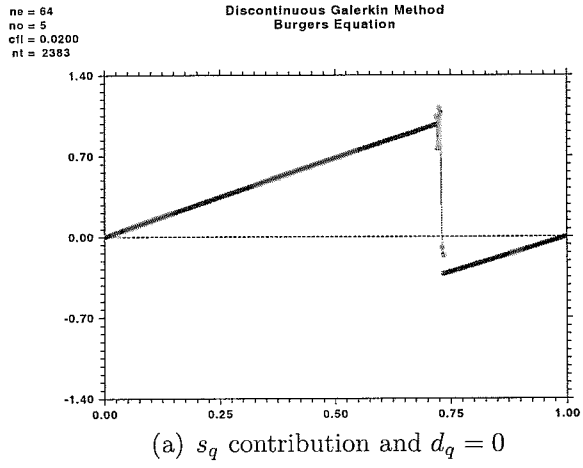


Figure 1.4: Burgers equation: zoom on the discontinuity of the 1D-domain $x = [0, 1]$ subdivided into 64 elements, \mathbb{P}_5 solutions top and \mathbb{P}_{19} bottom.

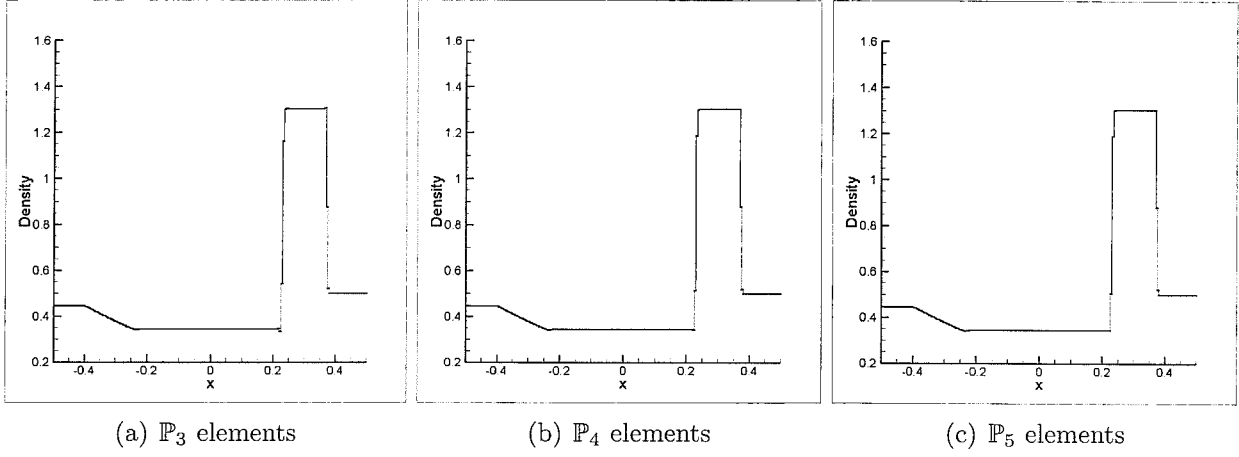


Figure 1.5: Lax problem, solution at $t = 0.15$, 200 elements. Lines connect average values within elements.

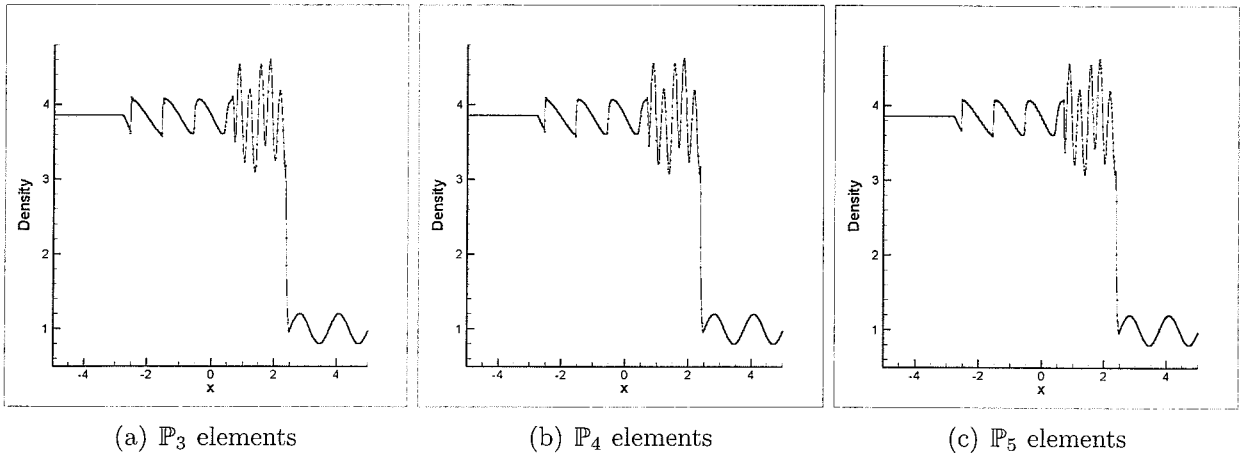


Figure 1.6: Shu-Osher problem, solution at $t = 1.8$, 200 elements. Lines connect $k + 1$ plotting points for each \mathbb{P}_k element.

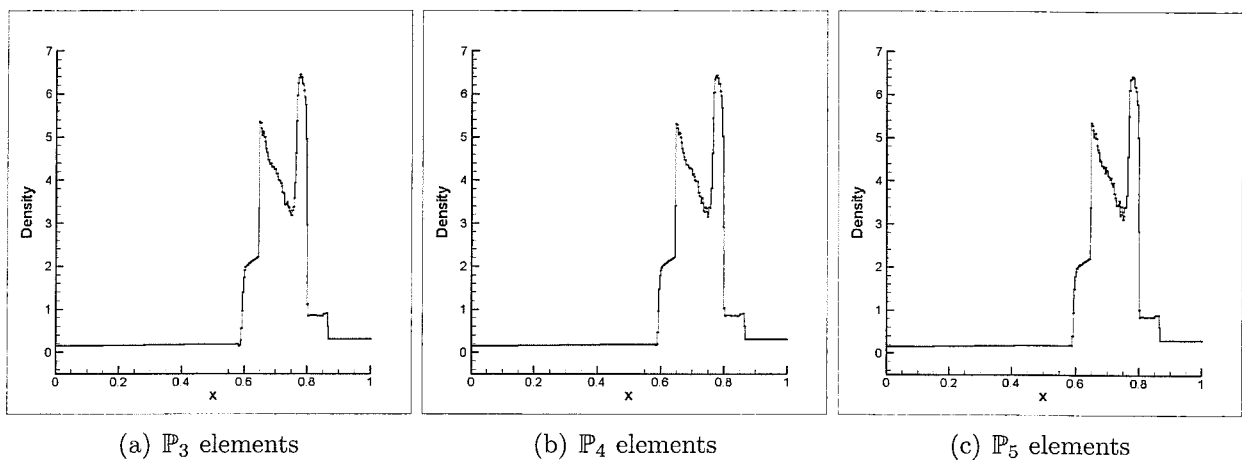


Figure 1.7: Blast waves interaction problem, $t = 0.038$, 400 elements. Lines connect average values within elements.

Bibliography

- [1] BASSI, F., AND REBAY, S. Accurate 2D Euler computations by means of a high order discontinuous finite element method. vol. 453 of *Lecture Notes in Physics*, Springer, pp. 234–240. XIV ICNMF, Bangalore, India, 11–15 July 1994.
- [2] BASSI, F., REBAY, S., MARIOTTI, G., PEDINOTTI, S., AND SAVINI, M. A high-order accurate discontinuous finite element method for inviscid and viscous turbomachinery flows. In *2nd European Conference on Turbomachinery Fluid Dynamics and Thermodynamics* (Antwerpen, Belgium, March 5–7 1997), R. Decuyper and G. Dibelius, Eds., Technologisch Instituut, pp. 99–108.
- [3] HARTMANN, R. Adaptive discontinuous Galerkin methods with shock-capturing for the compressible Navier-Stokes equations. *Int. J. Numer. Meth. Fluids* 51 (2006), 1131–1156.
- [4] HARTMANN, R., AND HOUSTON, P. Adaptive discontinuous Galerkin finite element methods for the compressible Euler equations. *J. Comput. Phys.* 183 (2002), 508–532.
- [5] JAFFRE, J., JOHNSON, C., AND SZEPESSY, A. Convergence of the discontinuous Galerkin finite element method for hyperbolic conservation laws. *Math. Models Methods Appl. Sci.* 5, 3 (1995), 367–386.
- [6] HANSBO, P. Explicit streamline diffusion finite element method for the compressible Euler equations in conservation variables *J. Comput. Phys.* 109, (1993), 274–288.
- [7] WOODWARD, P., AND COLELLA, P. The numerical simulation of two dimensional fluid flow with strong shocks. *J. Comput. Phys.* 54 (1984), 115–173.
- [8] SHI, J. ZHANG, Y.T. AND SHU, C.W. Resolution of high order WENO schemes for complicated flow structures. *J. Comput. Phys.* 186 (2003), 690–696.

F Bassi Shock capturing:

There are basically 3 terms to compute..

$$1) \vec{b} = \frac{\nabla p}{|\nabla p| \tau \epsilon}$$

$$2) dg = \sum_{k=1}^{n_{pld}} \frac{\partial g}{\partial u_h^k} \vec{\nabla} \cdot (E, F)_k$$

$$3) \xi_g = \frac{|dg|}{|g|} \cdot \frac{|\nabla p|}{p} \left(\frac{h_k}{\text{ord} + 1} \right)$$

Here we follow Bassi, Let

1) It is obvious

2) Let $g = P$ - the pressure then $\vec{\nabla} \cdot (E, F) = \frac{\partial E}{\partial u^1} \frac{\partial u^1}{\partial x} + \frac{\partial F}{\partial u^1} \frac{\partial u^1}{\partial y}$

$$dp = \sum_{k=1}^{n_{pld}} \frac{\partial p}{\partial u_h^k} \vec{\nabla} \cdot (E, F)_k$$

$$\left(\frac{\partial E}{\partial u^1} \right) = \begin{bmatrix} 0 & -(\gamma-3)u & 0 \\ (\frac{\gamma-3}{2})u^2 + (\frac{\gamma-1}{2})v^2 & -(\gamma-3)u & 0 \\ -uv & \frac{u^2}{(\gamma-1)} + (\frac{3}{2}-\gamma)u^2 + \frac{1}{2}v^2 & -uv \\ -\frac{u^2}{(\gamma-1)} + (\frac{1}{2}\gamma-1)(u^3+v^2u) & \frac{u^2}{(\gamma-1)} + (\frac{3}{2}-\gamma)u^2 + \frac{1}{2}v^2 & -uv \end{bmatrix}$$

$$\frac{\partial F}{\partial u^1} = \begin{bmatrix} 0 & 0 & 0 \\ -uv & \frac{u^2}{(\gamma-1)} + (\frac{3}{2}-\gamma)u^2 + \frac{1}{2}v^2 & \gamma v \\ (\frac{\gamma-3}{2})v^2 + (\frac{\gamma-1}{2})u^2 & -uv(\gamma-1) & \gamma v \\ -\frac{uv^2}{(\gamma-1)} + (\frac{1}{2}\gamma-1)(u^3+v^3) & -uv(\gamma-1) & \gamma v \end{bmatrix}$$

Artificial Viscosity for Discontinuous Solutions using DG-FEM

Here in we will follow a highly modified form of the method proposed by Persson and Pericci, 06.

Consider the Navier-Stokes equations

$$\frac{\partial \vec{q}}{\partial t} + \vec{\nabla} \cdot (\vec{F}_c - \vec{F}_v) = 0$$

To this set of equations we proposed to add another diffusive flux \vec{F}_{av} , giving

$$\frac{\partial \vec{q}}{\partial t} + \vec{\nabla} \cdot (\vec{F}_c - \vec{F}_v - \vec{F}_{av}) = 0$$

The ? is what should \vec{F}_{av} be.

Answer:

I want \vec{F}_{av} to be an anisotropic Laplacian term.

If we call that
$$\vec{F}_v = \begin{bmatrix} [G_{11}] & [G_{12}] \\ [G_{21}] & [G_{22}] \end{bmatrix} \begin{Bmatrix} \frac{\partial q}{\partial x} \\ \frac{\partial q}{\partial y} \end{Bmatrix}$$

Where G_{ij} is of size $n \times n$, then we will write

\vec{F}_{av} as

$$\vec{F}_{av} = \begin{bmatrix} [G_{11}^{av}] & [0] \\ [0] & [G_{22}^{av}] \end{bmatrix} \begin{Bmatrix} \frac{\partial q}{\partial x} \\ \frac{\partial q}{\partial y} \end{Bmatrix}$$

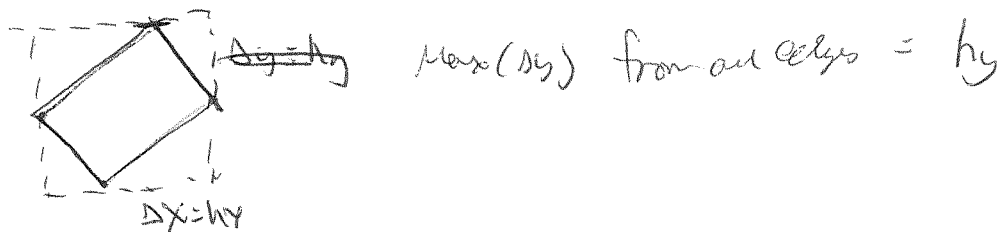
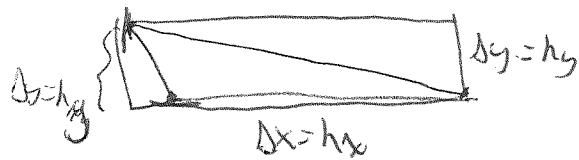
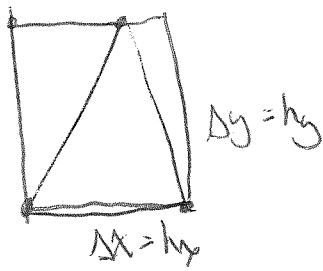
$$G_{ij} = \sum_{k=1}^{N_{max}} \frac{h_{x_i}}{N_{max}} \frac{h_{x_j}}{(P+1)} \begin{bmatrix} 1 & 0 & 0 & 0 & 0 & 0 \\ 0 & 1 & 0 & 0 & 0 & 0 \\ 0 & 0 & 1 & 0 & 0 & 0 \\ \frac{\partial q}{\partial x} & \frac{\partial q}{\partial y} & \frac{\partial q}{\partial x} & \frac{\partial q}{\partial y} & \frac{\partial q}{\partial x} & \frac{\partial q}{\partial y} \\ 0 & 0 & 0 & 0 & 1 & 0 \\ 0 & 0 & 0 & 0 & 0 & 1 \end{bmatrix} \text{ for two nodes}$$

$N_{max} = |V| + C$
 $N_{max} = |V| + C$

h_{x_1} is the x-component of enclosing quad of shape.

h_{x_2} is the y-component of enclosing quad

Graphical Detail of h_x, h_y .



I.E. take the longest edge's Δx and Δy measurements that gives h_x, h_y .

Remarks on the general A.V form

$$\vec{F}_{av} = \begin{bmatrix} [G_{11}^{av}] \\ [G_{22}^{av}] \end{bmatrix} \begin{Bmatrix} \frac{\partial \phi}{\partial x} \\ \frac{\partial \phi}{\partial y} \end{Bmatrix}$$

$$G_{ic}^{av} = \epsilon \lambda_{max}^i \frac{h_{xi}}{(p+1)} \begin{bmatrix} 1 & 0 & 0 & 0 & \dots \\ 0 & 1 & 0 & 0 & \dots \\ 0 & 0 & 1 & 0 & \dots \\ 0 & 0 & 0 & 1 & \dots \\ \vdots & \vdots & \vdots & \vdots & \ddots \end{bmatrix}$$

The energy equation's ~~temp~~ diffusion is $\sim \frac{\partial \rho H}{\partial x}$ not $\frac{\partial \rho E}{\partial x}$

this is to aid in total enthalpy preservation

λ_{max} has a direction as does the h_{xi} term this is to allow for anisotropic diffusion.

Discontinuity Detection using Pressure:

In previous notes it was always assumed that the detector was based on one of flow field quantities. Experimentation has shown that better discontinuity detection can be done if pressure is the indicator qty. Thus for the Mean flow we will base the indicator on the pressure

$$S_K = \int_{\Omega} \frac{(P - \hat{P})^2}{P^2} d\Omega \quad \text{where} \quad P = \rho(\gamma-1) \left(E - \frac{1}{2} (U^2 + V^2) \right)$$

$$\rho = \sum_{j=1}^N \tilde{\rho}_j \phi_j, \text{ etc.}$$

$$\hat{P} = \hat{\rho}(\gamma-1) \left(E - \frac{1}{2} (U^2 + V^2) \right)$$

$$\hat{\rho} = \sum_{j=1}^{N_{p-1}} \hat{\rho}_j \phi_j$$

No longer can this be represented by using the $\{\hat{g}\}^T [M] \{g\}$ relation thus a linearization of the indicator is formed and stored as well. the definitions of ε and all other things remain the same.

PDE Based artificial Diffusion:

To increase artificial diffusion we will appeal to the PDE-based method of Benter and Darmofal.

①

$$F_i^{av}(\vec{u}, \nabla \vec{u}) = A_{ij}^E \frac{\partial u}{\partial x_j}$$

$$A_{ij}^E = \hat{\epsilon}(\epsilon) \begin{bmatrix} [I] h_x & 0 \\ 0 & [I] h_y \end{bmatrix}$$

$$\bar{h} = \sum_{i=1}^d h_i$$

For 2D flow $[I] = \begin{bmatrix} 1 & 0 & 0 & 0 \\ 0 & 1 & 0 & 0 \\ 0 & 0 & 1 & 0 \\ 0 & 0 & 0 & 1 \end{bmatrix}$ 4x4 identity

This can be re-written as

$$F_i^{av} = \hat{\epsilon}(\epsilon) \frac{h_i}{\bar{h}} \frac{\partial u}{\partial x_i} \quad \text{No sum.}$$

$$\vec{u} = \begin{Bmatrix} p \\ p u_i \\ p H \end{Bmatrix} \rightarrow \text{use Helmholtz}$$

$$Q = .01 \Delta t$$

$$\epsilon \leq Q_L$$

$$Q_H = \frac{\lambda_{max}}{P}$$

$$\hat{\epsilon}(\epsilon) = \begin{cases} 0 & \epsilon \leq Q_L \\ \frac{1}{2} Q_H \left[\sin\left(\pi \left\{ \frac{\epsilon - Q_L}{Q_H - Q_L} - \frac{1}{2} \right\}\right) + 1 \right] & Q_L \leq \epsilon \leq Q_H \\ Q_H & \epsilon \geq Q_H \end{cases}$$

ϵ comes from the transport PDE

$$\frac{\partial \epsilon}{\partial t} = \nabla \left(\frac{\eta}{L} \nabla \epsilon \right) + \frac{1}{L} \left[\frac{\bar{h}}{P} \lambda_{max} S_K - \epsilon \right]$$

$$\tau = \frac{\min_i h_i}{C_1 P \lambda_{max}} \quad C_1 = 3$$

$$\eta = C_2 \begin{bmatrix} h_x^2 & 0 \\ 0 & h_y^2 \end{bmatrix} \quad \frac{\eta}{L} = \frac{C_1 C_2 P \lambda_{max}}{\min_i h_i} \begin{bmatrix} h_x^2 & 0 \\ 0 & h_y^2 \end{bmatrix}, \quad C_1 C_2 = 15$$

$$\text{Let } \bar{\epsilon} = \frac{\epsilon}{\alpha \omega L_r}$$

Now we can non-dimensionalize the A.V. PDE

$$\frac{\partial \bar{\epsilon}}{\partial \bar{t}} = \frac{1}{L_r} \nabla \left(\frac{C_1 C_2 P \lambda_{max}}{\min_i h_i} \begin{bmatrix} h_x^2 & 0 \\ 0 & h_y^2 \end{bmatrix} \frac{1}{L_r} \nabla \bar{\epsilon} \right) + \frac{C_1 P \lambda_{max}}{\min_i h_i} \left[\frac{\bar{h}}{P} \lambda_{max} S_K - \bar{\epsilon} \right]$$

Non-dimensional Form.

$$\frac{\partial \bar{\epsilon}}{\partial \bar{t}} = \nabla \left(\frac{C_1 C_2 P \lambda_{max}}{\min_i h_i} \begin{bmatrix} h_x^2 & 0 \\ 0 & h_y^2 \end{bmatrix} \nabla \bar{\epsilon} \right) + \frac{C_1 P \lambda_{max}}{\min_i h_i} \left[\frac{\bar{h}}{P} \lambda_{max} S_K - \bar{\epsilon} \right]$$

Discretization

$$\int_{\Omega} \phi_i \frac{\partial \varepsilon}{\partial \sigma} d\Omega = \int_{\Omega} \phi_i \nabla \cdot \left(\frac{c_1 c_2 \rho \tilde{\lambda}_{max}}{\min_i h_i} \begin{bmatrix} \tilde{h}_x^2 & 0 \\ 0 & \tilde{h}_y^2 \end{bmatrix} \nabla \varepsilon \right) + \phi_i \frac{c_1 \rho \tilde{\lambda}_{max}}{\min_i h_i} \left[\frac{\tilde{h}}{\rho} \tilde{\lambda}_{max} S_k - \varepsilon \right]$$

$$\bar{F}_x = \frac{c_1 c_2 \rho \tilde{\lambda}_{max}}{\min_i h_i} \tilde{h}_x^2 \frac{\partial \varepsilon}{\partial x}$$

$$\bar{F}_y = \frac{c_1 c_2 \rho \tilde{\lambda}_{max}}{\min_i h_i} \tilde{h}_y^2 \frac{\partial \varepsilon}{\partial y}$$

Using these:

$$\begin{aligned} \int_{\Omega} \phi_i \frac{\partial \varepsilon}{\partial \sigma} d\Omega &= \int_{\Omega} -\nabla \phi_i \cdot (\bar{F}_x, \bar{F}_y) + \phi_i \frac{c_1 \rho \tilde{\lambda}_{max}}{\min_i h_i} \left[\frac{\tilde{h}}{\rho} \tilde{\lambda}_{max} S_k - \varepsilon \right] d\Omega \\ &= \int_{\partial \Omega} \phi_i \{ \bar{F}_x n_x + \bar{F}_y n_y \} dS = \int_{\partial \Omega} \left(\frac{c_1 c_2 \rho \tilde{\lambda}_{max}}{\min_i h_i} \right) \left(\tilde{h}_x^2 \frac{\partial \varepsilon}{\partial x} \right) n_x + \left(\tilde{h}_y^2 \frac{\partial \varepsilon}{\partial y} \right) n_y dS \\ &\quad + \int_{\partial \Omega} \phi_i \left\{ \frac{c_1 c_2 \rho \tilde{\lambda}_{max}}{\min_i h_i} \left(\tilde{h}_x^2 \right) \left[\varepsilon \right] n_x + \left\{ \frac{c_1 c_2 \rho \tilde{\lambda}_{max}}{\min_i h_i} \tilde{h}_y^2 \right\} \left[\varepsilon \right] n_y dS \right\} \end{aligned}$$

Boundary Conditions:

Walls.

$$\frac{\partial \varepsilon}{\partial \hat{n}} = 0$$

Far field

$$\frac{\partial \varepsilon}{\partial \hat{n}} = \frac{\varepsilon_{\infty} - \varepsilon}{L}, \quad L = 10 h_i n_i = 10 (h_x n_x + h_y n_y), \quad \varepsilon_{\infty} = 0$$

$$\frac{\partial \varepsilon}{\partial \hat{n}} = \frac{0 - \varepsilon}{10(h_x n_x + h_y n_y)} = \frac{-\varepsilon}{10(h_x n_x + h_y n_y)}$$

The viscous flux on the Boundary

$$\int_{\partial \Omega} \phi_i (F_x^v(u^v, v^v) n_x + F_y^v(u^v, v^v) n_y) dS \quad \nabla u^v =$$

$$= \bar{F}_x^v n_x + \bar{F}_y^v n_y = \frac{c_1 c_2 \rho \tilde{\lambda}_{max}}{\min_i h_i} \tilde{h}_x^2 n_x \frac{\partial \varepsilon}{\partial x} + \frac{c_1 c_2 \rho \tilde{\lambda}_{max}}{\min_i h_i} \tilde{h}_y^2 n_y \frac{\partial \varepsilon}{\partial y}$$

To implement this we'll put the transport equation into a new artificial diffusion flow scheme. (3)

The final discretized system:

$$\int \phi_i \frac{\partial \xi}{\partial t} d\Omega - \int_{\Omega} -\nabla \phi_i \cdot (F_x, F_y) + \phi_i \frac{c_1 P \tilde{\lambda}_{max}}{minchi} \left[\frac{h \tilde{\lambda}_{max}}{P} S_K - \xi \right] d\Omega$$

$$- \int_{\partial \Omega_{int.}} \phi_i \{ F_x n_x + F_y n_y \} ds - \int_{\partial \Omega} \frac{1}{2} \left(\frac{c_1 c_2 P \tilde{\lambda}_{max}}{minchi} h_x^2 \frac{\partial \phi_i}{\partial x} \right) \llbracket \xi \rrbracket n_x +$$

$$\frac{1}{2} \left(\frac{c_1 c_2 P \tilde{\lambda}_{max}}{minchi} h_y^2 \frac{\partial \phi_i}{\partial y} \right) \llbracket \xi \rrbracket n_y ds + \int_{\partial \Omega} \left\{ \frac{c_1 c_2 P \tilde{\lambda}_{max}}{minchi} h_x^2 \right\} \llbracket \xi \rrbracket n_x +$$

$$\left\{ \frac{c_1 c_2 P \tilde{\lambda}_{max}}{minchi} h_y^2 \right\} \llbracket \xi \rrbracket n_y ds$$

1) Neumann bndy $\frac{\partial \xi}{\partial n} = 0$ walls

$$\int_{\partial \Omega} \phi_i \{ F_x n_x + F_y n_y \} ds = 0$$

2) Robin bndy $\frac{\partial \xi}{\partial n} = \frac{\sigma - L}{10 \cdot h \cdot n}$

$$\int_{\partial \Omega} \phi_i \left(\frac{c_1 c_2 P \tilde{\lambda}_{max}}{minchi} \right) h_x^2 \frac{\partial \xi}{\partial x} n_x + \phi_i \left(\frac{c_1 c_2 P \tilde{\lambda}_{max}}{minchi} \right) h_y^2 \frac{\partial \xi}{\partial y} n_y ds$$

The S_K detector src term:

The detector is processed to create S_K

$$S_K(F_K, \theta_s, \psi_0, \Delta\psi) = \begin{cases} 0 & F_K \leq \psi_0 - \Delta\psi \\ \theta_s & F_K \geq \psi_0 + \Delta\psi \\ \frac{\theta_s}{2} \left(1 + \sin\left(\pi \frac{(F_K - \psi_0)}{\Delta\psi}\right) \right) & |F_K - \psi_0| < \Delta\psi \end{cases}$$

F_K - is either resolution $\log_{10} \left(\frac{\langle f - \hat{f}_i, f - \hat{f} \rangle}{\langle \hat{f}_i, \hat{f} \rangle} \right)$

or jump

$$\frac{1}{|\partial \Omega_K|} \int_{\partial \Omega_K} \left| \frac{\llbracket P_{pressure} \rrbracket}{\{ P_{pressure} \}} \right| ds$$

$$\psi_0 = (4 + 4 \cdot \sigma / \sigma_0 d(\sigma))$$

$$\Delta\psi = 1.5$$

$$F_K \leq \psi_0 - \Delta\psi$$

$$F_K \geq \psi_0 + \Delta\psi$$

Remoder: Note that the $\frac{\text{AnomH}}{P}$ scaling is carried in the Σ computation. We could divide by $\frac{\text{AnomH}}{P}$ in the AN. PDE but that doesn't really matter. Just note that the AN. flux ~~to~~ will have no explicit scaling in it. (4)

The SK source term:

I want to control the on/off properties of the src term. From the input file these modifications will be made to Baster's switching f'n.

Baster's f'n

$$S_k(F_k; \theta_s, \psi_0, \Delta\psi) = \begin{cases} 0 & F_k \leq \psi_0 = \Delta\psi \\ \theta_s & F_k \geq \psi_0 + \Delta\psi \\ \frac{\theta_s}{2} \left(1 + \sin\left(\pi \frac{(F_k - \psi_0)}{2\Delta\psi}\right) \right) & |F_k - \psi_0| \leq \Delta\psi \end{cases}$$

width of bump

The original way of perenn and perenn tied the width $\Delta\psi$ to the value of F_k where it comes on. Baster has decoupled this.

To control source from input file the following is done.

$$\psi_0 = -(k + G_0 \log_{10}(P))$$

$\Delta\psi = .5$ - As Baster has it. Now we can control influence of P and the baseline value at which indication comes on. Note that $\Delta\psi = .5$ corresponds to a very sharp rise in viscosity. Hypothetically this is what Baster had in mind. Also $\theta_s = E_0$ from input file. Again more control.

Dual Consistency of Artificial Diffusion

This is analyzed using a Model PDE which is a non-linear poisson equation with Diffusion coefficient $\gamma(u, \nabla u)$ and source $S(u, \nabla u)$.

Model eqn:

$$\begin{aligned} -\nabla(\gamma(u, \nabla u) \nabla u) &= S(u, \nabla u) \quad \vec{x} \in \Omega \\ \text{subject to } u &= a, \quad \vec{x} \in \Gamma^D \\ \nabla u \cdot \vec{n} &= b, \quad \vec{x} \in \Gamma^N \end{aligned}$$

Continuous Adjoint.

Define a functional

$$J(u) = \int_{\Omega} j_{\Omega}(u) \, d\Omega + \int_{\Gamma^D} j_D(u) \, ds + \int_{\Gamma^N} j_N(u) \, ds$$

In this case Let $U = \nabla \nabla u \cdot \vec{n}$ then

$$\begin{aligned} J'[u](w) &= \int_{\Omega} j'_{\Omega}(u) w \, d\Omega + \int_{\Gamma^D} j'_D(u) (V_1 \nabla w + \gamma_{10} \nabla u + \gamma_{10} \nabla u \nabla u) \cdot \vec{n} \, ds \\ &\quad - \int_{\Gamma^N} j'_N(u) (\nabla \nabla w + \gamma_{20} \nabla u + \gamma_{20} \nabla u \nabla u) \cdot \vec{n} \, ds \\ &= J'_{\Omega}(u) + J'_{\Gamma}(u) \end{aligned}$$

← last 2 terms here

Take Frechet Deriv of PDE

$$-\frac{\partial}{\partial u} (\nabla \gamma \nabla u + \gamma \nabla u) = -[\gamma \nabla^2 w + \gamma_{10} \nabla u \cdot \nabla w + \gamma_{20} \nabla u \cdot \nabla w \nabla u] = S_u w + S_v$$

Continuous Adjoint is found by integration by parts

$$\begin{aligned} \int_{\Omega} -\psi [\nabla \cdot (\gamma \nabla w) + \gamma_{10} \nabla u \cdot \nabla w + \nabla \cdot (\gamma_{20} \nabla u \nabla w)] - \psi S_u w - \psi S_v \cdot \nabla w \, d\Omega \\ = \int_{\Omega} -\nabla \psi \cdot [\gamma \nabla w + \gamma_{10} \nabla u w] + \nabla \cdot (\gamma_{20} \nabla u \nabla w) - \psi S_u w + \nabla \psi \cdot S_v w \, d\Omega \\ + \oint_{\Gamma} -\psi [\gamma \nabla w + \gamma_{10} \nabla u w + \gamma_{20} \nabla u \nabla w] \cdot \vec{n} - \psi S_v w \cdot \vec{n} \, ds \end{aligned}$$

can go with $(\nabla \psi \cdot \nabla \gamma_{20})$

IBP Again gives

$$\begin{aligned} \int_{\Omega} \psi \nabla \cdot [\gamma \nabla \psi + \nabla \cdot (\gamma_{20} \nabla u \nabla \psi) + \nabla \cdot (\gamma_{10} \nabla u \psi)] - \psi S_u w + \nabla \psi \cdot S_v w \, d\Omega \\ + \oint_{\Gamma} -\psi [\gamma \nabla w + \gamma_{10} \nabla u w + \gamma_{20} \nabla u \nabla w] \cdot \vec{n} - \psi S_v w \cdot \vec{n} + \gamma \nabla \psi \cdot \vec{n} - \gamma_{10} \\ + \gamma_{20} \nabla \psi \cdot \nabla w \cdot \vec{n} \, ds \end{aligned}$$

Collecting terms

$$\int_{\Omega} \omega \left[\nabla \cdot (\gamma \nabla \psi) - \nabla \cdot (\psi \gamma_0 \nabla u) + \nabla \cdot (\gamma_0 \nabla \psi \nabla u) - \psi S_0 + \nabla \psi \cdot S \nabla u \right] d\Omega$$

$$+ \int_{\Gamma} \psi \left[\gamma \nabla \omega + \gamma_0 \nabla u \omega + \gamma_0 \cdot \nabla \omega \nabla u \right] \cdot \vec{n} - \psi S_0 \omega \cdot \vec{n} + \gamma \nabla \psi \omega \cdot \vec{n} + \gamma_0 \cdot \nabla \psi \nabla u \omega \cdot \vec{n} d\Gamma$$

Recall the Adjoint Identity Based on Duality.

$$J'_{\text{Euler}}(\omega) = \langle \omega, j_{\text{Euler}} \rangle_{\Omega} + \langle (C'_{\text{Euler}}) \omega, S_0'(\psi) \rangle =$$

$$\underbrace{\langle \omega, (N'_{\text{Euler}})^* \psi \rangle_{\Omega}}_{\text{Volume part}} + \langle (C'_{\text{Euler}}) \omega, (B'_{\text{Euler}})^* \psi \rangle_{\Gamma} = \underbrace{\langle N'_{\text{Euler}}, \psi \rangle_{\Omega}}_{\text{Volume part}} +$$

$$\langle B'_{\text{Euler}} \omega, (C'_{\text{Euler}})^* \psi \rangle_{\Gamma}$$

① Volume part implies.

$$(N'_{\text{Euler}})^* = -\nabla(\gamma \nabla \psi) + \nabla \cdot (\psi \gamma_0 \nabla u) - \nabla \cdot (\nabla \psi \cdot \gamma_0 \nabla u) - \psi S_0 + \nabla \psi \cdot S \nabla u$$

$$= j_{\text{Euler}}$$

② Dirichlet B.C.
 $\Gamma_D: B\omega = \omega$ Means the terms that involve ω by itself will define $(C'_{\text{Euler}})^*$ are ones in the inner product.

$$+ \gamma \nabla \psi \cdot \vec{n} - \gamma_0 \nabla u \psi + \gamma_0 \cdot \nabla \psi \nabla u \cdot \vec{n} \Rightarrow j_D = \psi \text{ on } \vec{x} \in \Gamma_D$$

$$[C'_{\text{Euler}}]^* = \gamma \nabla(\cdot) \cdot \vec{n} - \gamma_0 \nabla(\cdot) + \gamma_0 \cdot \nabla(\cdot) \nabla u \cdot \vec{n}$$

$$B^* \psi = \psi \quad C'_{\text{Euler}} \omega = -[\gamma \nabla \omega \cdot \vec{n} + \gamma_0 \omega \nabla u \cdot \vec{n} + \gamma_0 \cdot \nabla \omega \nabla u \cdot \vec{n}]$$

③ Neumann B.C.
 $\Gamma_N: B\omega = \gamma \nabla \omega \cdot \vec{n} \Rightarrow (C'_{\text{Euler}})^* \psi = \gamma \nabla \psi$

$$B^* \psi = \gamma \nabla \psi \cdot \vec{n} \quad C'_{\text{Euler}}(\omega) = \gamma_0 \omega \nabla u \cdot \vec{n} + \gamma_0 \cdot \nabla \omega \nabla u \cdot \vec{n}$$

Hence

$$\gamma \nabla \psi \cdot \vec{n} = j'_N \text{ on } \Gamma_N$$

$$\psi = j'_D \text{ on } \Gamma_D$$

Consistency Analysis:

(3)

$$N(u_h, v_h) = - \sum_{e \in \mathcal{E}_h} \int_{\Omega_e} \nabla \nabla u_h \cdot \nabla v_h - v_h S \, d\omega + \sum_{i \in \mathcal{I}_h} \int_{\Omega_i} \{ \nabla \nabla u_h \} \cdot [\![u_h]\!] + \{ \nabla \nabla v_h \} \cdot [\![u_h]\!] - \mu \{ v \} [\![u_h]\!] \cdot [\![v_h]\!] \, ds +$$

$$\sum_{e \in \mathcal{B}_h} \int_{\Gamma_0} \gamma^b \nabla u_h^+ \cdot \vec{n} \, v_h^+ + \gamma^b \nabla v_h^+ (u - a) \cdot \vec{n} - \mu \gamma^b (u - a) \, v_h^+ \, ds +$$

$$\sum_{e \in \mathcal{B}_h} \int_{\Gamma_w} \gamma^b \nabla u_h \, v_h^+ \, ds = 0$$

Linearize this

$$N'_{[U]}(u_h, v_h) \equiv - \sum_{e \in \mathcal{E}_h} \int_{\Omega_e} \nabla \nabla u_h \cdot \nabla v_h + \nabla u_h \nabla u_h \cdot \nabla v_h + (\nabla u_h \cdot \nabla u_h) (\nabla u_h \cdot \nabla v_h) - v_h S \nabla u_h +$$

$$\sum_{i \in \mathcal{I}_h} \int_{\Omega_i} [\{ \nabla \nabla u_h \} + \{ \nabla u_h \nabla u_h \} + \{ \nabla u_h \cdot \nabla u_h \nabla u_h \} - \mu \{ \gamma^b \} [\![u_h]\!] - \mu \{ \gamma^b u_h \} [\![u_h]\!] - \mu \{ \gamma^b \nabla u_h \} \cdot [\![u_h]\!] \cdot [\![v_h]\!] +$$

$$\{ \nabla \nabla v_h \} [\![u_h]\!] + \{ \nabla u_h \nabla v_h \} \cdot [\![u_h]\!] + \{ \nabla u_h \cdot \nabla u_h \nabla v_h \} \cdot [\![u_h]\!] \, ds$$

$$+ \sum_{e \in \mathcal{B}_h} \int_{\Gamma_0} \left[\gamma^b \nabla u_h^+ \cdot \vec{n} + \gamma^b u_h^+ \nabla u_h^+ \cdot \vec{n} + \gamma^b \nabla u_h^+ \cdot \nabla u_h^+ - \mu \gamma^b u_h^+ (u_h^+ - a) - \mu \gamma^b \nabla u_h^+ (u_h^+ - a) \right] v_h^+ +$$

$$\gamma^b \nabla v_h^+ (u_h^+ \cdot \vec{n}) + \gamma^b u_h^+ \nabla v_h^+ (u_h^+ - a) \cdot \vec{n} + \gamma^b \nabla u_h^+ \cdot \nabla v_h^+ (u_h^+ - a) \, ds$$

$$+ \sum_{e \in \mathcal{B}_h} \int_{\Gamma_w} \gamma^b \nabla u_h + \gamma^b u_h^+ \gamma^b v_h^+ + \gamma^b \nabla u_h^+ \nabla v_h^+ \, ds$$

Define

$$N'_{[U]}(u_h, \psi_h) \equiv N'_{[S]}(u_h, \psi_h) + N'_{[U]}(u_h, \psi_h) + N'_{[V]}(u_h, \psi_h)$$

$$N'_{E\cup\Omega}(w_h, \psi_h) \equiv - \sum_{e \in \mathcal{E}^h} \int_{\Omega_e} \gamma \nabla w_h \cdot \nabla \psi_h + \gamma_0 w_h \nabla u_h \cdot \nabla \psi_h + (\gamma_{\partial\Omega} \cdot \nabla w_h)(\nabla \psi_h \cdot \vec{n}) - \psi_h S_{\partial\Omega} w_h - \psi_h S_{\partial\Omega} \cdot \nabla w_h \, ds$$

I.B.P

$$= \sum_{e \in \mathcal{E}^h} \int_{\Omega_e} w_h \left[\nabla \cdot (\gamma \nabla \psi_h) - \gamma_0 \nabla u_h \cdot \nabla \psi_h + \nabla \cdot (\gamma_{\partial\Omega} \cdot \nabla \psi_h \nabla u_h) \right] + \psi_h S_{\partial\Omega} w_h - \int_{\partial\Omega} \nabla \psi_h \cdot S_{\partial\Omega} u_h \, ds + \int_{\partial\Omega} -\gamma \nabla \psi_h^+ \cdot \vec{n} w_h^+ - \gamma_{\partial\Omega} \cdot \nabla \psi_h^+ \nabla u_h^+ \cdot \vec{n} + \psi_h^+ S_{\partial\Omega} w_h^+ \cdot \vec{n} \, ds + \sum_{b \in \mathcal{B}^h} -\gamma^b \nabla \psi_h^+ \cdot \vec{n} w_h^+ - \gamma_{\partial\Omega}^b \cdot \nabla \psi_h^+ \nabla u_h^+ \cdot \vec{n} + \psi_h^+ S_{\partial\Omega} w_h^+ \cdot \vec{n} \, ds$$

Ignoring the Surface terms

Let $\psi_h \rightarrow \psi$, $u_h \rightarrow u$ gives

$$\sum_{e \in \mathcal{E}^h} \int_{\Omega_e} w_h \left[\nabla \cdot (\gamma \nabla \psi) - \nabla \cdot (\psi \gamma_0 \nabla u) + \nabla \cdot (\gamma_{\partial\Omega} \cdot \nabla \psi \nabla u) \right] + \nabla \psi \cdot S_{\partial\Omega} w_h \, ds = S'_{\partial\Omega} w_h \quad \text{by definition}$$

Interior Surface terms

$$N'_{E\cup\Omega}(w_h, \psi_h) \equiv \sum_{e \in \mathcal{E}^h} \int_{\partial\Omega_e} \left[\frac{1}{2} \gamma \nabla w_h^+ + \frac{1}{2} \gamma_0 w_h^+ \nabla u^+ + \frac{1}{2} \gamma_{\partial\Omega} \cdot \nabla w_h^+ \nabla u^+ - \mu \frac{1}{2} \gamma \llbracket w_h \rrbracket - \mu \frac{1}{2} \gamma_0 w_h \llbracket u_h \rrbracket - \mu \frac{1}{2} \gamma_{\partial\Omega} \cdot \nabla w_h \llbracket u_h \rrbracket \right] \cdot \llbracket \psi_h \rrbracket - \gamma \nabla \psi_h^+ \cdot \vec{n} w_h^+ - \gamma_{\partial\Omega} \cdot \nabla \psi_h^+ \nabla u_h^+ \cdot \vec{n} w_h^+ + \psi_h^+ S_{\partial\Omega} w_h^+ \cdot \vec{n} + \{ \gamma \nabla \psi_h \} u_h^+ \cdot \vec{n} + \{ \gamma_0 w_h \nabla \psi_h \} \cdot \llbracket u_h \rrbracket + \{ \gamma_{\partial\Omega} \cdot \nabla w_h \nabla \psi_h \} \cdot \llbracket u_h \rrbracket$$

Using $\gamma \nabla \psi_h^+ \cdot \vec{n} w_h^+ = \{ \gamma \nabla \psi_h \} \cdot \vec{n} u_h^+ + \frac{1}{2} \llbracket \gamma \nabla \psi_h \rrbracket w_h^+$ gives

$$N'_{E\cup\Omega}(w_h, \psi_h) = \sum_{e \in \mathcal{E}^h} \int_{\partial\Omega_e} \left[\frac{1}{2} \gamma \nabla w_h^+ \cdot \vec{n} \right] \cdot \llbracket \psi_h \rrbracket - \{ \gamma \nabla \psi_h \} \cdot \vec{n} w_h^+ - \frac{1}{2} \llbracket \gamma \nabla \psi_h \rrbracket w_h^+ - \gamma_{\partial\Omega} \cdot \nabla \psi_h^+ \nabla u_h^+ \cdot \vec{n} w_h^+ + \psi_h^+ S_{\partial\Omega} w_h^+ \cdot \vec{n} + \{ \gamma \nabla \psi_h \} u_h^+ \cdot \vec{n} + \{ \gamma_0 w_h \nabla \psi_h \} \cdot \llbracket u_h \rrbracket + \{ \gamma_{\partial\Omega} \cdot \nabla w_h \nabla \psi_h \} \cdot \llbracket u_h \rrbracket \, ds$$

Let $\psi_h \rightarrow \psi$, $u_h \rightarrow u$ then $\llbracket \psi_h \rrbracket = 0$, $\llbracket u_h \rrbracket = 0$

$$N'_{\text{FW}}(\omega_n, \psi) = \sum_{\alpha \in \mathcal{A}_h} \int_{\partial \Omega_\alpha} (-\nabla \psi \cdot \nabla \psi \cdot \vec{n} + \psi \nabla \psi \cdot \vec{n}) \omega_n ds \quad (5)$$

On the Boundaries

[illegible]

Let $\psi_h \rightarrow \psi$, and $\psi_h^w \rightarrow 0$ the $\psi_h|_{\Gamma_D} \rightarrow a$, $\psi_h|_{\Gamma_D} \rightarrow \int_{\Delta} [\psi]$

$$\nabla \psi \cdot \vec{n} \Big|_{\Gamma_N} \rightarrow j'_{\Gamma_N}, \quad \nabla u \cdot \vec{n} \Big|_{\Gamma_N} \rightarrow a_N \quad \text{thus}$$

$$N'_{b[\nu]}(\omega_h, \psi) = \sum_{\delta \in B_L} \int_{\Gamma_D} \omega_i \left[j'_D - \mu v^b \omega_h j'_D + v^b_{\Gamma_D} \cdot \nabla \psi \nabla \omega_h \cdot \vec{n} \omega_h \right. \\ \left. + \psi_h \nabla_{\Gamma_D} \vec{n} \omega_h \right] ds + \int_{\Gamma_W} v^b_{\Gamma_D} \omega_h \nabla \psi + \nabla_{\Gamma_D} \psi \omega_h \nabla \psi^+ ds$$

[illegible]

$$N'_{\text{DQ}}(\psi, \psi) = 0 + \int_{\text{cont}} \int_{\text{surf}} \left(-\nabla \psi \cdot \nabla \psi \nabla \psi \cdot \vec{n} + \psi \nabla \psi \cdot \vec{n} \right) ds + \int_{\text{DQ}} \left(-\nabla \psi \cdot \nabla \psi \nabla \psi \cdot \vec{n} + \psi \nabla \psi \cdot \vec{n} \right) ds$$

Proof of $O(h^2)$ Behavior of functional convergence.

1) Todd Oliver's way. I write this because I get a bit confused and his explanation is lacking in sufficient detail to explain it. Thus I will show it with the necessary detail so that I understand it.

Consider a ~~linear~~ bi-linear functional i.e. linear in both arguments

$$B(u, v) = \ell(v) \quad \forall v \in V \quad \text{where } u \text{ and } v \text{ are both } \in V$$

The corresponding dual problem (See earlier notes on Dual consistency) $\psi \in V$

$$B(u, \psi) = J(u) \quad \forall u \in V \quad \text{i.e. } u \text{ is test fn here this is very important.}$$

The discrete problem is find $u_h \in V_h$ such that

$$B_h(u_h, v_h) = \ell(v_h) \quad \forall v_h \in V_h$$

The discrete dual problem is find $\psi_h \in V_h$ such that

$$B_h(u_h, \psi_h) = J(u_h) \quad \forall u_h \in V_h$$

We wish to form the error in fn based on the exact vs discrete solutions i.e. $J(u) - J(u_h)$ if $u \in V$ and $u_h \in V_h$ are the solutions (which they are).

Clearly $J(u) = B(u, \psi)$ and $B_h(u_h, \psi_h) = J(u_h)$

Assume then that u, ψ satisfy the Bilinear operator,

$$B_h(u, \psi) = B(u, \psi) \quad \text{i.e. the discrete Bilinear operator is consistent.}$$

$$J(u) - J(u_h) = B(u, \psi) - B_h(u_h, \psi_h)$$

$$J(u) - J(u_h) = B_h(u, \psi) - B_h(u_h, \psi_h)$$

7 What is asymptotic behavior of $J(u) - J(u_h)$

6

Begin with

$$J(u) - J(u_h) = B_h(u, \psi) - B_h(u_h, \psi_h)$$

Add zero as $B_h(u_h, \psi) - B(u_h, \psi)$ gives

$$J(u) - J(u_h) = B_h(u, \psi) - B_h(u_h, \psi) + B(u_h, \psi) - B(u_h, \psi_h)$$

$$= B_h(u, \psi) + B(u_h, \psi - \psi_h) +$$

$$\text{Add zero as } B_h(u - u_h, \psi_h) - B_h(u - u_h, \psi_h)$$

$$J(u) - J(u_h) = B_h(u - u_h, \psi) + B_h(u_h, \psi - \psi_h) + B_h(u - u_h, \psi_h) - B_h(u - u_h, \psi_h)$$

$$J(u) - J(u_h) = \overset{\textcircled{1}}{B_h(u - u_h, \psi - \psi_h)} + \overset{\textcircled{2}}{B_h(u_h, \psi - \psi_h)} + \overset{\textcircled{3}}{B_h(u - u_h, \psi_h)}$$

Now we can't say anything about $\textcircled{1}$ quite yet But.

Recall $B_h(u, \psi) = J(u) \forall u \in V$ and $B_h(u, v) = \ell(v) \forall v \in V_h$

If $B_h(\cdot, \cdot)$ is consistent i.e. $B_h(u, v_h) = \ell(v_h) \forall v_h \in V_h$
and like wise dual consistency $\Rightarrow B_h(u_h, \psi) = \ell(u_h) \forall \psi \in V_h$

keeping this in mind.

$$\textcircled{1}: B_h(u_h, \psi - \psi_h) = B_h(u_h, \psi) - B_h(u_h, \psi_h)$$

$B_h(u_h, \psi_h) = J(u_h)$ by definition ~~Further~~ ~~that as~~

Further dual consistency $\Rightarrow B_h(u_h, \psi) = J(u_h) \forall \psi \in V_h$

$$\textcircled{1} \Rightarrow J(u_h) - J(u_h) = 0$$

$$\textcircled{3}: B_h(u - u_h, \psi_h) = B_h(u, \psi_h) - B_h(u_h, \psi_h) \quad \forall \psi_h \in V_h$$

Primal consistency $\Rightarrow B_h(u, \psi_h) = \ell(\psi_h) \forall \psi_h \in V_h$

and $B_h(u_h, \psi_h) = \ell(\psi_h)$ by definition. Thus

$$\textcircled{3} \Rightarrow \ell(\psi_h) - \ell(\psi_h) = 0$$

Thus

$$J(u) - J(u_h) = B_h(u - u_h, \psi - \psi_h) \quad \text{if consistent and dual consistent}$$

From Approximation theory of linear functionals in form type forms

$$|B_h(u-u_h, \psi-\psi_h)| \leq C \|u-u_h\| \|\psi-\psi_h\|$$

for $u \in V_h$ where V_h is complete up to order p then

$$\|u-u_h\| \leq C O(h^{p+1/2})$$

like wise $\psi_h \in V_h \Rightarrow \|\psi-\psi_h\| \leq C O(h^{p+1/2})$, $O(h^{p+1/2})$ is worse case.

thus

$$|J(u) - J(u_h)| \leq C O(h^{p+1/2}) O(h^{p+1/2}) = C O(h^{2p+1}) \approx \boxed{C O(h^{2p})}$$

This proof is not possible without the assumption of dual consistency.

2) There is a more intuitive way to arrive at this but it is actually harder to construct

Consider $J(u)$ again Linear

If we have a discrete solution $u_h \in V_h$ then the functional $J(u) \approx J(u_h) + \frac{\partial J}{\partial u}|_{u_h} (u-u_h)$

$$J(u) - J(u_h) = \frac{\partial J}{\partial u}|_{u_h} (u-u_h)$$

If we applied to the usual constraint equation, then

$$R(u) = 0 \approx R(u_h) + \frac{\partial R}{\partial u}|_{u_h} (u-u_h)$$

$$(u-u_h) \approx - \frac{\partial R}{\partial u}|_{u_h} (u_h)$$

results in..

$$\boxed{J(u) - J(u_h) = - \langle \psi, R_h(u_h) \rangle}$$

For a linear problem $R_h(u_h) = L(u_h - u)$ thus

$$J(u) - J(u_h) = - \langle \psi, L(u-u_h) \rangle$$

introduce $\psi = \psi - \psi_h + \psi_h$ gives

$$J(u) - J(u_h) = \langle \psi - \psi_h, L(u-u_h) \rangle + \langle \psi_h, L(u-u_h) \rangle$$

adding zero $\approx \langle \psi - \psi_h, L u_h \rangle + \langle \psi - \psi_h, L u_h \rangle$ gives

$$J(u) - J(u_h) = \langle \psi - \psi_h, L(u-u_h) \rangle + \langle \psi_h, L(u-u_h) \rangle + \langle \psi - \psi_h, L u_h \rangle - \langle \psi - \psi_h, L u_h \rangle$$

Expanding all but the first term. gives

(4)

$$J(u) - J(u_h) = \underbrace{\langle \psi - \psi_h, L(u - u_h) \rangle}_{(4)} + \underbrace{\langle \psi_h, L u \rangle}_{(1)} - \underbrace{\langle \psi_h, L u_h \rangle}_{(2)} \\ + \underbrace{\langle \psi, L u_h \rangle}_{(3)} - \underbrace{\langle \psi_h, L u_h \rangle}_{(1)} + \underbrace{\langle \psi_h, L u_h \rangle}_{(2)}$$

Now we don't want to do any subtraction or we'll just end up back where we started. The goal is to show how primal and dual consistency arise.

Primal consistency $B_h(u, \psi_h) = B_h(u_h, \psi_h) \Rightarrow \langle \psi_h, L u \rangle = \langle \psi_h, L u_h \rangle = Q(\psi_h)$

(1) $\rightarrow Q(\psi_h)$
 (2) $\rightarrow Q(\psi_h)$ } cancel.

(3), (4), (5), (6) Recall duality statement $\langle \psi, L^* u \rangle = \langle L^* \psi, u \rangle$

thus all of these can be written as

(2) $\rightarrow \langle L^* \psi, u_h \rangle$

(4) $\rightarrow \langle L^* \psi_h, u_h \rangle$

(5) $\rightarrow \langle L^* \psi, u_h \rangle$

(6) $\rightarrow \langle L^* \psi_h, u_h \rangle$

If the scheme is dual consistent the $\langle L^* \psi, u_h \rangle = \langle L^* \psi_h, u_h \rangle = J(u)$

thus

(3), (4), (5), (6) $\rightarrow J(u_h) - J(u_h) + J(u_h) - J(u_h) = 0$

$J(u) = J(u_h) = \langle \psi - \psi_h, L(u - u_h) \rangle$

again apply theory

$|J(u) - J(u_h)| \leq C \|\psi - \psi_h\| \|u - u_h\| \leq C O(h^{2p})$

This is just as nice as Oliver but comes from the Taylor series error estimator.

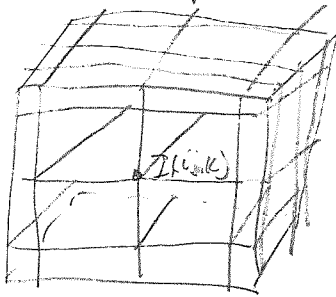
Nodal Quadrature

Consider $\frac{\partial \phi}{\partial t} + \nabla \cdot (F_x, F_y, F_z) = 0$ e.g. 3D Euler

If we have cartesian Hex than. $\frac{\partial f}{\partial x}, \frac{\partial f}{\partial y}, \frac{\partial f}{\partial z}$ are 1D and all others are zero.

Let the Basis ϕ_I be tensor products of Lagrange Polynomials then.

$\phi_I = l_{ijk}$ $I = (i-1)N_j + (j-1)N_k$ Then ϕ_I is the node I that corresponds to ijk is the structured grid within each element



Derive an element

$$\int_{\Omega_e} \phi_I \frac{\partial \phi}{\partial t} d\Omega_e - \int_{\Omega_e} \nabla \phi_I (F_x, F_y, F_z) d\Omega_e + \phi_I(t) = 0$$

$$\nabla \phi_I = \left(\frac{\partial \phi_I}{\partial x} \hat{x}, \frac{\partial \phi_I}{\partial y} \hat{y}, \frac{\partial \phi_I}{\partial z} \hat{z} \right)$$

$$\phi = \sum_I \phi_I$$

$$\int_{\Omega_e} \phi_I \sum_I \frac{\partial \phi}{\partial t} d\Omega_e - \int_{\Omega_e} \frac{\partial \phi_I}{\partial x} F_x(\phi) + \frac{\partial \phi_I}{\partial y} F_y(\phi) + \frac{\partial \phi_I}{\partial z} F_z(\phi) d\Omega_e$$

Mass Matrix

$$\int_{-1}^1 \int_{-1}^1 \int_{-1}^1 l_i(\xi) l_j(\eta) l_k(\zeta) \frac{\partial \phi}{\partial t} l_l(\xi) l_m(\eta) l_n(\zeta) |J| d\xi d\eta d\zeta$$

$$M_{IJ} = \int_{-1}^1 \int_{-1}^1 \int_{-1}^1 [l_i(\xi) l_j(\eta) l_k(\zeta)] [l_l(\xi) l_m(\eta) l_n(\zeta)] |J| d\xi d\eta d\zeta$$

$$= \left(\int_{-1}^1 l_i(\xi) l_l(\xi) d\xi \right) \left(\int_{-1}^1 l_j(\eta) l_m(\eta) d\eta \right) \left(\int_{-1}^1 l_k(\zeta) l_n(\zeta) d\zeta \right)$$

$$\delta_{ik} \delta_{jl} \delta_{mn} = \sum_p l_k(\zeta_p) l_n(\zeta_p) \omega_p \sum_q l_j(\eta_q) l_m(\eta_q) \omega_q \sum_r l_i(\xi_r) l_l(\xi_r) \omega_r = \delta_{ik} \delta_{jl} \delta_{mn}$$

$$= w_i w_j w_k : \left. \begin{array}{l} i=l \\ j=m \\ \text{and} \\ k=n \end{array} \right\} \text{All these have to be } \Rightarrow I=J$$

0 otherwise

Therefore the mass Matrix is Diagonal.

① Volume Residual

$$\int_{\Omega} \frac{\partial \phi}{\partial \xi} \xi_x F_x(\tilde{U}) + \frac{\partial \phi}{\partial \eta} \eta_y F_y(\tilde{U}) + \frac{\partial \phi}{\partial \zeta} \zeta_z F_z(\tilde{U}) d\Omega$$

X-term

$$\int_{-1}^1 \int_{-1}^1 \int_{-1}^1 \frac{\partial \phi_i(\xi)}{\partial \xi} \xi_x F_x(\tilde{U}(\xi, \eta, \zeta)) d\zeta d\eta d\xi \approx \sum_P \sum_B \sum_r \frac{\partial \phi_i(\xi_r)}{\partial \xi} \phi_j(\eta_B) \phi_k(\zeta_P)$$

$$F(\tilde{U}(\xi_r, \eta_B, \zeta_P)) w_r w_B w_P$$

$$\int_{-1}^1 \phi_k(\zeta) \left(\int_{-1}^1 \phi_j(\eta) \left(\int_{-1}^1 \frac{\partial \phi_i(\xi)}{\partial \xi} \xi_x F_x(\tilde{U}(\xi, \eta, \zeta)) d\xi \right) d\eta d\zeta \right)$$

$$\sum_P \phi_k(\zeta_P) w_P \sum_B \phi_j(\eta_B) w_B \sum_r \frac{\partial \phi_i(\xi_r)}{\partial \xi} \xi_x F_x(\tilde{U}(\xi_r, \eta_B, \zeta_P))$$

$$\tilde{U}(\xi_r, \eta_B, \zeta_P) = \tilde{U}_{rPq} \quad \tilde{U} \text{ at node } r, p, q \quad \phi_k(\zeta_P) = \delta_{kP} = \text{ones}$$

$$\delta_{kP} w_P \delta_{jB} w_B \sum_r \frac{\partial \phi_i(\xi_r)}{\partial \xi} \xi_x F_x(\tilde{U}_{rPq}) = w_k w_j \sum_r \frac{\partial \phi_i(\xi_r)}{\partial \xi} \xi_x F_x(\tilde{U}_{rjk})$$

y-term by analogous is

$$w_i w_k \sum_B \frac{\partial \phi_j(\eta_B)}{\partial \eta} \eta_y F_y(\tilde{U}_{ijk})$$

z-term by analogous is

$$w_i w_j \sum_P \frac{\partial \phi_k(\zeta_P)}{\partial \zeta} \zeta_z F_z(\tilde{U}_{ijP})$$

Cost of: prismatic residual evaluations

$$\sum_{j=1}^{p+1} \sum_{k=1}^{N_p} \nabla(\phi_i(\xi_k) \ell_j(\gamma)) [\vec{F}_c(u) - \vec{F}_v(u, \gamma_0)] |\Omega| d\xi_k d\gamma_j$$

$$\sum_{j=1}^{p+1} \sum_{k=1}^{N_p} \nabla(\phi_i \ell_j) \cdot [\vec{F}_c(u) - \vec{F}_v] |\Omega| \omega_k \omega_\ell$$

To obtain

$$U: U(\xi_k, \eta_k, \gamma_\ell) = \sum_{j=1}^{p+1} \sum_{l=1}^{N_p} \hat{O}_{ij} \phi_i(\xi_k, \eta_k) \ell_j(\gamma_\ell) = \sum_{l=1}^{N_p} \hat{O}_{il} \phi_i(\xi_k, \eta_k) \rightarrow \frac{(p+1)(p+2)}{2}$$

Less efficient pure mod $O_{U_M} = \frac{(p+1)^2 p+2}{2}$ $O_{U_N} = 1$

$$\nabla U: \nabla U(\xi_k, \eta_k, \gamma_\ell) = \sum_{j=1}^{p+1} \sum_{l=1}^{N_p} \hat{O}_{ij} (\phi_{i\xi} \ell_j + \phi_{i\eta} \ell_j + \phi_{i\gamma} \ell_j) = \sum_{l=1}^{N_p} \hat{O}_{il} (\phi_{i\xi}, \phi_{i\eta}) + \sum_{j=1}^{p+1} \sum_{l=1}^{N_p} \hat{O}_{ij} (\phi_i \ell_j)$$

$$\rightarrow O_{\nabla U} = \frac{(p+1)(p+2)}{2} \cdot 2 + \frac{(p+1)^2 p+2}{2}$$

$$O_{\nabla U_M} = \frac{(p+1)^2 p+2}{2} \cdot 3$$

Residual point: $O_{\nabla U_N} = 2 \cdot \frac{(p+1)(p+2)}{2} + (p+1)$

$$\nabla(\phi_i \ell_j) = (\phi_{i\xi} \xi_k \ell_j(\gamma_\ell) + \phi_{i\eta} \eta_k \ell_j(\gamma_\ell) + \phi_{i\gamma} \gamma_k \ell_j(\gamma_\ell) + \phi_{i\xi} \xi_j \ell_j(\gamma_\ell) + \phi_{i\eta} \eta_j \ell_j(\gamma_\ell) + \phi_{i\gamma} \gamma_j \ell_j(\gamma_\ell) + \phi_{i\xi} \xi_2 \ell_j(\gamma_\ell) + \phi_{i\eta} \eta_2 \ell_j(\gamma_\ell) + \phi_{i\gamma} \gamma_2 \ell_j(\gamma_\ell))$$

$$R = \sum_{j=1}^{p+1} \sum_{k=1}^{N_p} [\phi_{i\xi} \xi_k \ell_j(\gamma_\ell) + \phi_{i\eta} \eta_k \ell_j(\gamma_\ell) + \phi_{i\gamma} \gamma_k \ell_j(\gamma_\ell)] (\vec{F}_c - \vec{F}_v)$$

$$R: 3 \left[2 \left[\frac{(p+1)(p+2)}{2} [O_U + O_{\nabla U}] \right] + \frac{(p+1)^2 p+2}{2} [O_U + O_{\nabla U}] \right] \text{ per point}$$

$$O_R = 3 \left[2 \frac{(p+1)(p+2)}{2} [O_U + O_{\nabla U}] + \frac{(p+1)^2 p+2}{2} [O_U + O_{\nabla U}] \right]$$

$$\text{Total } V = O_R + \frac{(p+1)^2 p+2}{2}$$

$$O_{R_M} = 3 \left[3 \frac{(p+1)^2 p+2}{2} [O_{U_M} + O_{\nabla U_M}] \right] +$$

$$V_M = O_{R_M} + \frac{(p+1)^2 p+2}{2}$$

$$OR_N = 3 \left[2 \frac{(p+1)(p+2)}{2} [O_{UN} + O_{\sigma UN}] + (p+1) [O_{UN} + O_{\sigma UN}] \right]$$

Surface

Tri face

$$O_{UM} = \frac{(p+1)^2(p+2)}{2}$$

$$O_{\sigma UM} = 3 O_{UM}$$

$$O_U = \frac{(p+1)p+2}{2}$$

$$O_{\sigma U} = 2 \cdot O_U + \frac{(p+1)(p+2)}{2}$$

$$2 \cdot 3 = 18$$

$$3 \cdot \frac{(3)^4}{2} = 18$$

$$3 \cdot \frac{(3)(4)}{2} = 18$$

$$R: \phi_i F_c - \phi_i F_v - \nabla \phi_i S_{gm} + \phi_i \text{pen}$$

$$OR: 2 \left[\frac{(p+1)(p+2)}{2} \text{ points } \uparrow \text{ face} \right] [O_U + O_{\sigma U}] + 3 \frac{(p+1)(p+2)}{2} + \frac{(p+1)^2 p+2}{2}$$

$$OR_M: 2 \left[\frac{(p+1)p+2}{2} \text{ 2 face} \right] [O_{\sigma UM} + 3 O_{UM}] + 3 \frac{(p+1)(p+2)}{2} + \frac{(p+1)^2 p+2}{2}$$

$$OR_N: 2 \left[\frac{(p+1)(p+2)}{2} [O_{UN} + O_{\sigma UN}] + \frac{(p+1)(p+2)}{2} + 1 \right]$$

Quad Surface:

$$R: \phi_i F_c - \phi_i F_v - \nabla \phi_i S_{gm} + \phi_i \text{pen}$$

$$OR_i: 3 \left[(p+1)^3 [O_U + O_{\sigma U}] + \frac{(p+1)^2 \cdot 3}{2} + 3 \frac{(p+1)^2 p+2}{2} \right]$$

$$OR_M: 3 \left[(p+1)^3 [O_{UM} + 3 O_{\sigma UM}] + \frac{(p+1)^2 p+2}{2} \cdot 3 \right]$$

$$OR_N: 3 \left[(p+1)^3 [O_{UN} + 3 O_{\sigma UN}] + \frac{(p+1)^2 (p+1) \cdot 3}{2} \right]$$

Row Pivoting:

When pivoting the rows of a matrix one is essentially rearranging the equations. Such that if a matrix A is pivoted to get \tilde{A}

then

$$[A] \xrightarrow{\text{pvd}} [\tilde{A}] \text{ then } [A(i,:)] = [\tilde{A}(\text{pivot}(i),:)]$$

when solving $[A]x = \{b\}$ this has the important result that

$$\{x\} = [\tilde{A}]^{-1} \{b(\text{pivot})\}$$

For Matrix vector products

$$\{y\} = [A]\{x\}$$

$$\{y(\text{pivot})\} = \{\tilde{y}(\text{pivot})\} = [\tilde{A}]\{x\} \text{ or } \{y(\text{pivot})\} = [\tilde{A}]\{x\}$$

Therefore when doing LU-decomposition it's very important that the pivoting is implemented correctly for LU-matvec and for ilu and tri-diag factorizations Namely

$$[A]^{-1}[C] \Rightarrow [U]^{-1}[L]^{-1}[C] = \{c(\text{pivot})\} \text{ ie. } [L][U]\{c'\} = \{c(\text{pivot})\}$$

